Available online at www.sciencedirect.com
ScienceDirect
Journal of Catalysis 245 (2007) 259–266
JOURNAL OF CATALYSIS
www.elsevier.com/locate/jcat

The role of chlorine in the generation of catalytic active species located in Au-containing MCM-41 materials

I. Sobczak [a,*], A. Kusior [a], J. Grams [b], M. Ziolek [a]

[a] *Faculty of Chemistry, A. Mickiewicz University, Grunwaldzka 6, 60-780 Poznań, Poland*
[b] *Institute of General and Ecological Chemistry, Technical University of Łódź, Żeromskiego 116, 90-924 Łódź, Poland*

Received 30 August 2006; revised 10 October 2006; accepted 11 October 2006
Available online 14 November 2006

Abstract

Gold nanoparticles were generated inside silicate MCM-41 mesoporous materials by two methods, co-precipitation in the presence of a cationic surfactant (COP) and incipient wetness impregnation (IMP). The samples were characterized by XRD, nitrogen sorption, UV–vis, TEM, TOF-SIMS, and DTG/DTA methods and were tested in acetonylacetone (AcAc) cyclization/dehydration in the gas phase and NO reduction with propene in the presence of oxygen (NO-SCR) monitored by FTIR. Metallic gold was determined in both samples; as expected, its dispersion was lower on the impregnated material. In addition, Au species surrounded by chloride ions was generated in silicate MCM-41 matrix prepared by the one-step synthesis with Si (sodium silicate) and Au ($HAuCl_4$) sources. This sample revealed high activity in AcAc cyclization to MCP (methylcyclopentenone), demonstrating the basic character of the surface. The basicity of this catalyst results from the presence of chloride. Moreover, this catalyst exhibits excellent performance in the electron transfer to oxygen in the NO-SCR reaction. The role of chloride anions as promoters in this reaction is demonstrated.

Keywords: AuMCM-41; Chloride/TOF-SIMS; Acetonylacetone cyclization/dehydration; NO-SCR/FTIR

1. Introduction

Gold catalysts have been of a great interest in many laboratories and the industry since the 1980s [1,2]. At present, it is evident that the method used to introduce gold onto or inside an oxide support plays a crucial role in the metal dispersion, which is thought by many investigators to determine the catalytic activity in many gold-catalyzed reactions [3,4]. Among the various techniques applied for the introduction of gold, the co-precipitation (CP) and deposition–precipitation (DP) methods are recommended for the modification of oxide supports [1,4]. $HAuCl_4$ is the most frequently used gold source. Recently, mesoporous matrices with very high surface areas were intensively studied as supports for gold species [5–9]. Metallic gold is recognized as the main active species in many redox reactions [10]. The reduction of gold cations occurs at a relatively low temperature and even in air atmosphere [1,11].

Various parameters, including temperature and atmosphere of activation and reducibility of the support, have been already considered in the chemistry, structure, and catalytic activity of gold-containing solids [1,3,11,12]. However, to the best of our knowledge, there are no reports about the role of chloride ions in gold catalysts supported on MCM-41 mesoporous molecular sieves. Recently, the effect of chlorine in Au/CeO_2 [13] and $Au–Au^{+}–Cl_x/Fe(OH)_y$ ($x < 4$, $y \leqslant 3$) [14] was studied. In the first case, residual chlorine determines the strength of the Au/CeO_2 interaction and decreases the total and selective oxidation of CO. However, Qiao and Deng [14] showed that the notion that supported gold must be chloride-free may not be correct. They indicated that hydroxyl species in unwashed and uncalcined material $Au–Au^{+}–Cl_x/Fe(OH)_y$ ($x < 4$, $y \leqslant 3$) may weaken the interactions between Au species and Cl^{-}, thus resulting in sufficient high activity toward CO oxidation in the presence of large amount of chloride.

In this work we focus, for the first time, on the effect of chloride ions in gold surrounding in an MCM-41 matrix on the formation of species active in the acid–base and redox processes.

* Corresponding author.
E-mail address: sobiza@amu.edu.pl (I. Sobczak).

0021-9517/$ – see front matter
doi:10.1016/j.jcat.2006.10.014

For that purpose, gold was introduced into silicate MCM-41 mesoporous materials (1) via incipient wetness impregnation with hydrochloric acid (denoted as IMP) and (2) during synthesis of the MCM-41 sample, which is in effect co-precipitation in the presence of a template (denoted as COP). The prepared materials were tested in the acetonylacetone (AcAc) cyclization/dehydration reaction (acid–base test) and in the surface interactions between NO, O_2, and C_3H_6 (i.e., the mixture used in HC-SCR process).

2. Experimental

2.1. Catalyst preparation

Mesoporous molecular sieves of MCM-41 type were synthesized by the hydrothermal method [15]. Sodium silicate (27% SiO_2 in 14% NaOH; Aldrich) was used as a silicon source, and cetyltrimethylammonium chloride (Aldrich) was the surfactant template. The gel formed from these components (molar gel ratios = $1SiO_2$:0.75NaOH:6.5CTMACl:$0.075H_2SO_4$:$103.75H_2O$) was stirred for about 0.5 h. The pH was adjusted to 11, after which distilled water was added. The gel was loaded into a stoppered polypropylene (PP) bottle and heated without stirring at 373 K for 24 h. The mixture was then cooled to room temperature, and the pH level was adjusted to 11 with H_2SO_4. This reaction mixture was reheated to 373 K for 24 h to produce highly ordered samples. The resulting precipitated product was washed with distilled water and dried in air at ambient temperature, and the template was removed by calcination at 823 K for 2 h in helium flow, followed by 14 h in air under static conditions.

In the IMP approach, the Au/MCM-41 catalyst was prepared by incipient wetness impregnation of the MCM-41 support with $HAuCl_4$ (Johnson Matthey) with gold loading of 1 wt%. The amount of solution used was chosen in such a way that the liquid filled up only the pores of the mesoporous support. After this impregnation, the catalysts were dried at 373 K for 5 h and calcined at 773 K for 3 h in air.

In the COP technique, the direct synthesis of AuMCM-41 was performed in the same manner as conventional MCM-41. The only difference was the admission of $HAuCl_4$ as the source of gold into the gel containing sodium silicate (Si source) and the template (CTACl, cetyltrimethylammonium chloride). The Si/Au atom ratio was 256 (corresponding to 1 wt% of Au). This material is denoted as COP (co-precipitated).

2.2. XRD

The XRD patterns were obtained on a TUR-62 diffractometer using CuK_α radiation ($\lambda = 0.154$ nm), with a step size of 0.02° in the small-angle range and 0.05° in the high-angle range.

2.3. N_2 adsorption/desorption

The surface area and pore volume of the samples were measured by nitrogen adsorption at 77 K, using the conventional procedure on a Micromeritics 2010 apparatus. Before the adsorption measurements, the samples were degassed in vacuum at 573 K for 2 h.

2.4. TEM

For TEM measurements, powders were deposited on a grid with a holey carbon film and transferred to JEOL 2000 electron microscope operating at 80 kV.

2.5. DTA/DTG

Thermogravimetric measurements were carried out in air atmosphere using a SETARAM SETSYS-12 apparatus with a temperature ramp of 5 K min^{-1}.

2.6. TOF-SIMS

The time-of-flight secondary ion mass spectrometry (TOF-SIMS) investigations were performed using an ION-TOF instrument (TOF-SIMS IV) equipped with a 25-kV pulsed $^{69}Ga^+$ primary ion gun in the static mode. To obtain the plain catalyst surface, the powder samples were tableted before the measurements. The tablets were attached to the sample holder using a double-sided tape. For each sample, three spectra and images were collected (from different areas). The analyzed area corresponded to a square range of 500 × 500 to 200 × 200 μm. A pulsed electron flood gun was used for the charge compensation.

2.7. Acetonylacetone cyclization/dehydration

The catalysts were tested for acetonylacetone (AcAc) cyclization as the probe reaction. A tubular down-flow reactor was used in experiments that were carried out at atmospheric pressure, using nitrogen as the carrier gas. The catalyst bed (0.05 g) was first activated for 2 h at 723 K under nitrogen flow (40 cm^3 min^{-1}). Subsequently, a 0.5 cm^3 of acetonylacetone (Fluka, GC grade) was continuously passed over the catalyst at 623 K. The substrate was delivered with a pump system and vaporized before being passed through the catalyst with the flow of nitrogen carrier gas (40 cm^3 min^{-1}). The reaction products were collected for 30 min downstream of the reactor in the cold trap (solid CO_2) and analyzed by gas chromatography (GC 8000 Top equipped with a capillary column of DB-1, operated at 353 K, attached to a FID).

2.8. FTIR measurements

Infrared spectra were recorded with the Vector 22 (Bruker) spectrometer. The pressed wafers of the materials (∼5 mg cm^{-1}) were placed in a vacuum cell and activated at 723 K for 3 h under vacuum (0.04 mbar). The experiments were carried out in static conditions by various modes: (i) NO adsorption at room temperature (RT), followed by O_2 admission, C_3H_6 adsorption at RT, and heating at 523 and 623 K; (ii) C_3H_6 adsorption at RT, followed by O_2 admission and heating at 523 K, NO adsorption

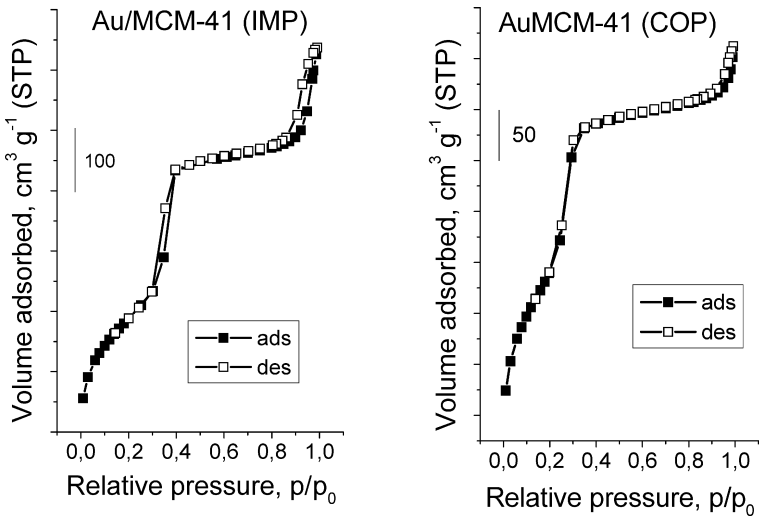

Fig. 1. N_2 adsorption/desorption isotherms of Au-containing MCM-41 materials.

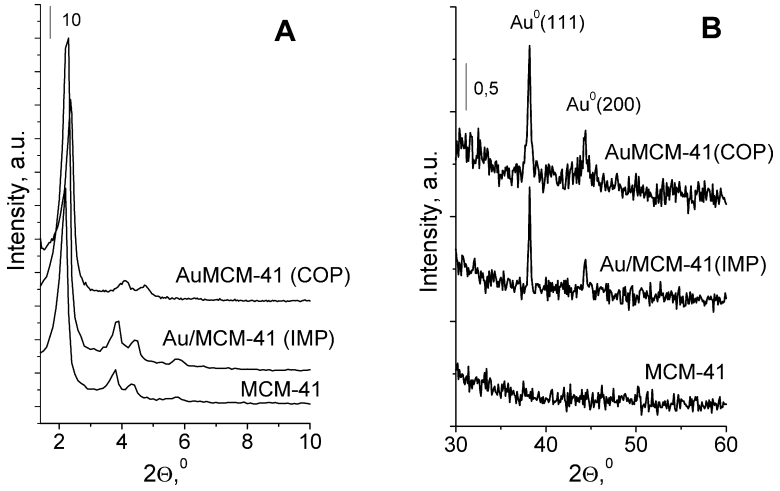

Fig. 2. XRD patterns of the catalysts: small-angle (A) and high-angle (B) XRD range.

at RT, and heating at 523 and 623 K; and (iii) saturation of the sample with oxygen at RT, followed by NO and C_3H_6 adsorption at RT. The spectra were recorded at room temperature. The spectrum without any sample ("background spectrum") was subtracted from all recorded spectra. The IR spectra of the activated samples were subtracted from those recorded after the adsorption of probe molecules followed by various treatments. The reported spectra are the results of this subtraction.

3. Results and discussion

Deposition–precipitation, co-precipitation, and phosphine grafting are the recommended methods for gold loading onto the metal oxide supports. These methods lead to much better gold dispersion than can be achieved by the conventional impregnation technique. This behavior is commonly recognized as a key factor in the activity of gold catalysts. In this work, we consider the role of another factor: the residual chlorine. For that purpose, we characterized two samples: (i) a material prepared by the incipient wetness impregnation method, designated Au/MCM-41(IMP), and (ii) a catalyst synthesized by the co-precipitation technique in the presence of the cationic surfactant, designated AuMCM-41(COP).

3.1. Catalyst characterization

The nitrogen adsorption/desorption isotherms of both gold catalysts (Fig. 1) are typical of nanostructured materials (type IV according to the IUPAC classification), with the inflection point at p/p_0 between 0.2 and 0.4, depending on the sample. Not only these N_2 sorption isotherms, but also small-angle X-ray diffraction (XRD) patterns (Fig. 2A), indicate that texture and structure parameters of the prepared catalysts depend on the method used for introducing Au. Both types of materials exhibit hexagonally ordered mesopores, with AuMCM-41(COP) having a lower surface area, pore diameter, and adsorption volume than Au/MCM-41(IMP) (Table 1). Metallic gold crystallites are formed on both materials, with their size determined by the method of Au introduction. The size of Au crystallites in AuMCM-41(COP) was estimated as 3–18 nm, based on TEM images (not shown here). Gold particles on TEM pictures of Au/MCM-41(IMP) exhibit diverse dimensions and shapes (es-

Table 1
Characterization of the samples

Catalyst	Surface area BET ($m^2\ g^{-1}$)	Pore volume (ads.) ($cm^3\ g^{-1}$)	Average pore diam. (ads.) (nm)	Au size (from TEM) (nm)
MCM-41	1076	1.25	3.90	–
Au/MCM-41(IMP)	1049	1.23	3.92	Difficult to determine
AuMCM-41(COP)	886	0.81	2.94	3–18

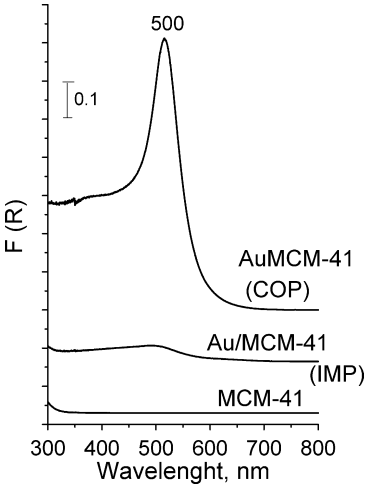

Fig. 3. UV–vis spectra of the catalysts.

pecially for agglomerates), making it difficult to estimate their sizes. However, the peaks at $2\Theta = 38.2°$ from Au(111) and at 44.8° from Au(200) in the high-angle XRD patterns [7,10,16], shown in Fig. 2B, are sharper for the impregnated material, suggesting larger Au agglomerates in the impregnated sample. The same can be concluded from the more intense ultraviolet–visible (UV–vis) [16] band at 500 nm for AuMCM-41(COP) (Fig. 3). Moreover, this feature was confirmed by TOF-SIMS showing a higher intensity ratio of Au_3^-/Au^- for Au/MCM-41(IMP) (Table 2) and the TOF-SIMS images (Fig. 4).

The most important finding from this work is the presence of chloride ions in the surrounding of gold centres in the mesoporous catalysts detected by TOF-SIMS. These chloride ions have a great impact on the catalytic activity of the samples (Table 2). The intensity ratio of chloride ions to the total number of ions is approximately one order of magnitude higher for AuMCM-41(COP) than for Au/MCM-41(IMP). The presence of chloride ions is important in conjunction with their location. The $AuCl^-/Au^-$ intensity ratio gives information about

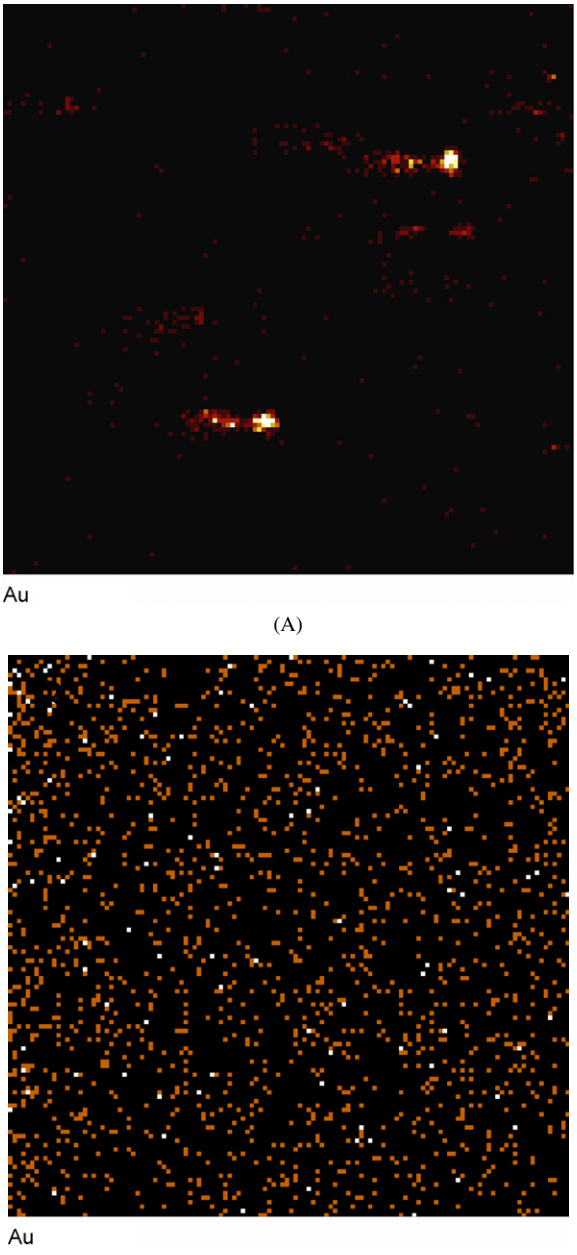

Fig. 4. TOF-SIMS images (200 × 200 μm) of Au/MCM-41(IMP) (A) and AuMCM-41(COP) (B) catalysts. Bright color indicates Au ions.

the amount of gold bonded to or surrounded by chloride ions. $AuCl^-$ is not detected for Au/MCM-41(IMP), whereas the $AuCl^-/Au^-$ intensity ratio for AuMCM-41(COP) is very high. Interestingly, the $AuCl^-/Au^-$ intensity ratio is much lower in

Table 2
TOF-SIMS results and catalytic activity in AcAc reaction (623 K)

Catalysts	TOF-SIMS Cl^-/total	TOF-SIMS $AuCl^-/Au^-$	TOF-SIMS Au_3^-/Au^-	AcAc conv. (%)	AcAc reaction MCP/DMF*
MCM-41	–	–	–	30	0.095
Au/MCM-41(IMP)	0.0019	No signal	0.30	35	0.080
AuMCM-41(COP)	0.015	1.46	0.12	38	104
AuMCM-41(COP) as made (with template)	0.061	0.19	0.11	–	–

* Reaction products: MCP—methylcyclopentenone, DMF—dimethylfuran.

the as-made material still containing the surfactant (template), indicating that calcination causes formation of the Au–Cl bond. It is important to stress that besides Au–Cl species, metallic gold is also present in the catalyst (Figs. 2B and 3). The calcination does not lead to agglomeration of metallic gold species (i.e., the Au_3^-/Au^- intensity ratio does not increase). Note that in TOF-SIMS, ions indicating Au–O bonding were not emitted; this supports the finding of chloride surrounding gold species. In contrast to these results, direct evidence of AuO^-, AuO_2^-, and $AuOH^-$ ions clusters on Au/Al_2O_3 and Au/TiO_2 catalysts was reported by TOF-SIMS in another study [17].

The difference in the residual chloride between the samples with Au introduced during the synthesis and by a postsynthesis method is attributed to the interaction of the Au source with the template. The cationic surfactant (cetyltrimethylammonium cations) interacts with a part of $[AuCl_4]^-$ ions from $HAuCl_4$ and stabilizes Au–Cl species. During calcination, the surfactant is eliminated while Au–Cl species become incorporated into the walls of the MCM-41 material. This results in a changed appearance of small-angle XRD patterns (Fig. 2A).

This is not the case with the postsynthesis treatment of the mesoporous support with $HAuCl_4$. The $[AuCl_4]^-$ species incorporated that way are not stabilized in the template-free silicate MCM-41 structure and during calcination are easily decomposed with the formation of HCl and/or Cl_2. The DTA/DTG analyses support this conclusion. The DTG curve of the uncalcined AuMCM-41(COP) shows the weight loss at 335 K from H_2O desorption, subsequent two minima at 500 and 610 K typical of the template removal [18] from silicate MCM-41, and an additional minimum at 750 K (Fig. 5) accompanied by an exothermic effect registered on the DTA curve.

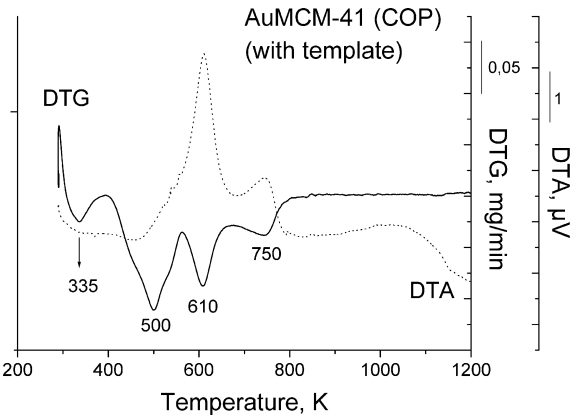

Fig. 5. DTA/DTG profiles of AuMCM-41(COP) catalyst.

The latter is most probably due to the decomposition of the template associated with the $[AuCl]_4^-$ ions. This behavior is not observed with calcined samples and with Au/MCM-41(IMP).

3.2. Acetonylacetone transformation

To gain insight into the effect of Au–Cl species on the catalytic activity, we examined two reactions: acetonylacetone (AcAc) cyclization and dehydration performed at 623 K in the gas phase, and selective catalytic reduction of NO (NO-SCR) with propene in the presence of oxygen. The data given in Table 2 demonstrate a significant influence of the catalyst preparation procedure on selectivity in AcAc cyclization and dehydration. It is known [19,20] that in this reaction, dimethylfuran (DMF) is produced on Brønsted acid centres, whereas Brønsted basic centres are involved in the formation of methylcyclopentenone (MCP) (see Scheme 1). It has been established that

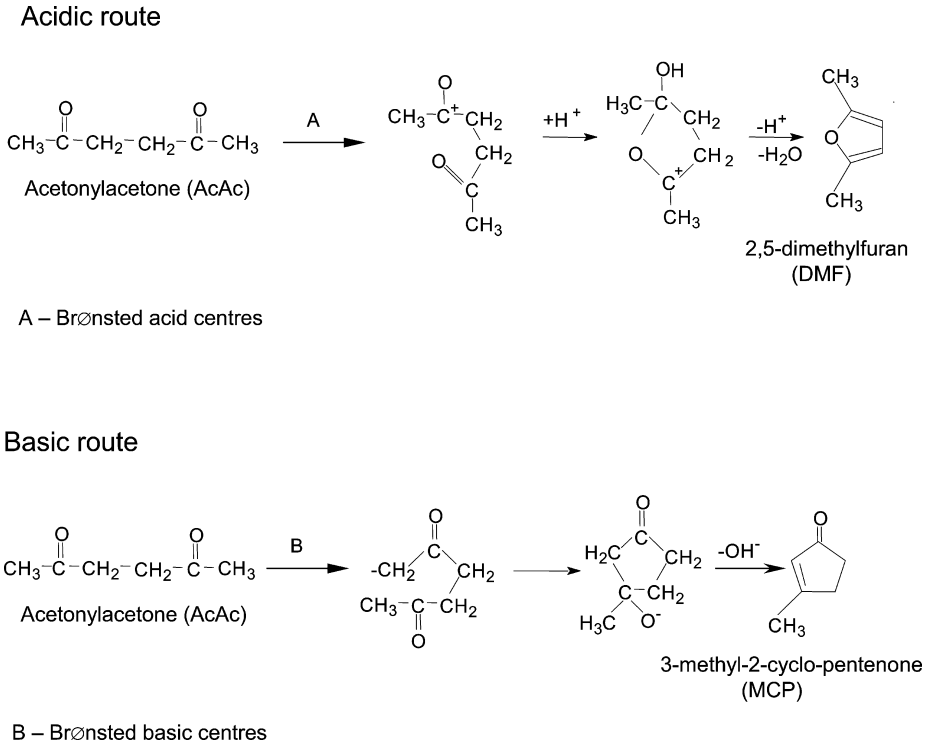

Scheme 1. Scheme of acetonylacetone (AcAc) transformation.

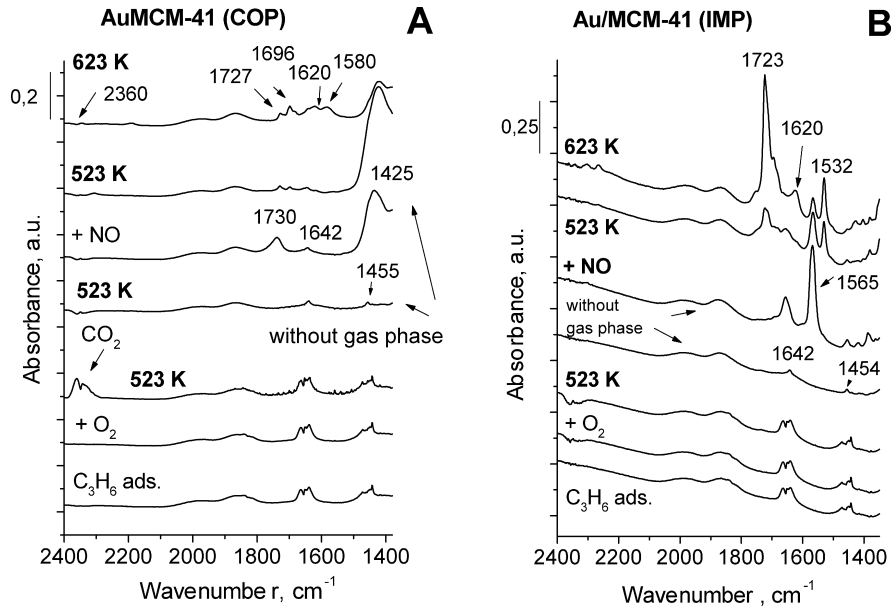

Fig. 6. FTIR spectra of AuMCM-41(COP) (A) and Au/MCM-41(IMP) (B) materials after the admission of reagents at RT in the following order: C_3H_6, O_2, heating at 523 K, NO introduction and heating at 523 and 623 K.

the selectivities MCP/DMF $\gg 1$ characterize basic properties of the catalyst, whereas MCM/DMF $\ll 1$ indicates acidic character of the material. If this ratio is $\sim$1, then the acid–basic character of the catalyst can be concluded. It is often reported that OH^- groups are responsible for these active sites. However, both of the catalysts used in this work exhibit almost the same amount of OH groups, as judged from the IR spectra ($\sim$3740 cm^{-1}). The main difference between Au/MCM-41(IMP) and AuMCM-41(COP) is due to the various amount of chloride. Taking this into account, there is no doubt that the presence of Au–Cl species is responsible for a very high basicity of AuMCM-41(COP), leading to a very high MCP selectivity (MCP/DMF = 104). The observed difference in the conversion of AcAc [from 35% for the impregnated sample to 38% for AuMCM-41(COP)] is negligible and could be caused by small differences in the texture parameters of the materials and the size of Au metal particles. However, the dramatic changes in reaction selectivity could not be due to the textural differences, because these features are not responsible for basicity. The selectivity changes clearly originate from the presence of chloride ions.

3.3. FTIR study of NO, O_2, C_3H_6 adsorption and co-adsorption

Gold centres supported on various metal (Fe, Zn, Mg, Ti, Al) oxides are active catalysts for the reduction of NO with propene/O_2/moisture [4,21]. Therefore, various gold catalysts have been tested in this reaction or studied using NO adsorption and FTIR techniques [9]. Some important processes relevant to this activity are HC-SCR (selective catalytic reduction of NO with hydrocarbons) and the NO_x-trap process. The use of a NO_x-trap catalyst infers that the engine operates alternatively under lean and rich atmospheres; during the lean period, NO_x molecules present in the exhaust gas are oxidized to NO_2 by Pt [30,31] and stored on the catalyst, whereas during rich spikes, the atmosphere is driven fuel rich for a brief time to reduce NO_x to N_2. For the HC-SCR process, generally two reaction pathways are considered [32]:

$$\text{(i) } \mathrm{CH} \xrightarrow{\mathrm{O_2}} \mathrm{HC{-}O} \xrightarrow{\mathrm{NO}} \mathrm{N_2 + CO_2 + H_2O}$$

and

$$\text{(ii) } \mathrm{NO} \xrightarrow{\mathrm{O_2}} \mathrm{NO_2} \xrightarrow{\mathrm{HC}} \mathrm{N_2 + CO_2 + H_2O}.$$

The reaction route depends on the composition of the catalysts.

To estimate the adsorption and catalytic behavior of the prepared materials in the NO reduction with propene FTIR investigations were performed. The experiments were carried out in a vacuum cell, in which pressed wafers of the sample were placed and NO, O_2, and C_3H_6 were added in various sequences and compositions. The results of these experiments are shown in Figs. 6–8. The infrared band assignment is consistent with finding in our earlier studies and the published literature [22–29].

Fig. 6 displays the FTIR spectra after admission of reagents in the following order: C_3H_6, O_2, and NO into AuMCM-41(COP) (Fig. 6A) and Au/MCM-41(IMP) (Fig. 6B) samples. Propene is weakly chemisorbed or physisorbed at RT on the surface of both catalysts, as shown by the bands at $\sim$1640 cm^{-1} (ν C=C) and the several bands in the 1450–1390 cm^{-1} range (ν =CH_2 and =CH physisorbed and weakly chemisorbed on various centers). Admission of O_2 and heating at 523 K do not change the FTIR spectra of the impregnated material, indicating that the oxidation of C_3H_6 does not occur under these conditions. In contrast, the same treatment of AuMCM-41(COP) leads to complete oxidation of propene to CO_2 (evidenced by the bands at $\sim$2360 cm^{-1}). Weakly chemisorbed propene is observed on the surface (the spectra resulted from subtraction of the gas phase) of both catalysts after these procedures (the bands at 1642 and 1455 cm^{-1}).

The admission of NO at RT onto the Au/MCM-41(IMP) sample is followed by partial oxidation of propene to carboxylate species (the band at 1572 cm^{-1}, ν COO^- in acetate), which transforms to carbonates (1534 cm^{-1}) and acetone (ν C=O at 1727 cm^{-1} from physisorbed acetone and a shoulder at 1690 cm^{-1} from acetone hydrogen bonded to hydroxyl groups) at 523 K. This means that on this catalyst, the NO molecules promote partial oxidation of propene, whereas in the case of AuMCM-41(COP) material, the promoter is already present on the catalyst surface. Taking into account the above TOF-SIMS evidence for the presence of chloride in this catalyst, it can be concluded that chloride ions take part in electron transfer during oxidation of propene with oxygen to CO_2 without the presence of NO molecules. Exposure of AuMCM-41(COP) pretreated with propene and oxygen to NO produces intense bands at 1730 and 1425 cm^{-1}, originating from NO_2^- species chemisorbed on gold. The first band can be also due to dinitrosyl species or acetone, but the second one at 1425 cm^{-1} is attributed to nitrite species. The production of nitrites proves the presence of active oxygen ions, which could result from the electron transfer from chloride to oxygen. Nitrites react at 623 K with chemisorbed propene to oxygenates (1696, 1580 cm^{-1}), NO_2 (1620 cm^{-1}) CO, and CO_2 (2150 and 2360 cm^{-1}, respectively).

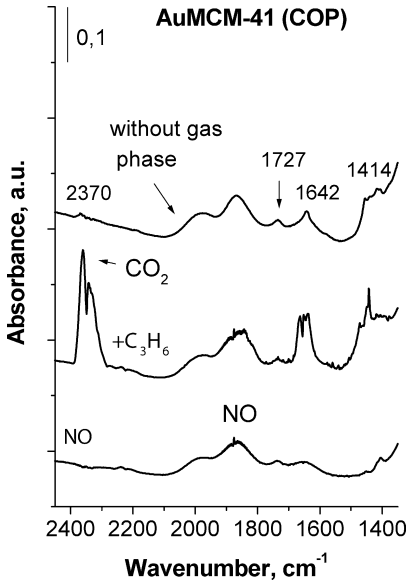

Fig. 7. FTIR spectra of AuMCM-41(COP) saturated with oxygen at RT and after the admission of NO and C_3H_6 at RT.

Saturation of the AuMCM-41(COP) sample with oxygen at RT is followed by the admission of NO and propene causes C_3H_6 oxidation already at RT (Fig. 7). An intense band from the gaseous CO_2 can be seen, and the chemisorbed propene and nitrites can be observed in the spectrum without the gas phase. Nitrite species are formed after the adsorption of NO on the oxygen-saturated sample (weak bands at ca 1730 and 1430 cm^{-1}). The same series of experiments performed on Au/MCM-41(IMP) showed no activity of the sample.

When a different sequence of reagent admission is applied (NO, followed by O_2 and then propene), the difference between the interaction with both catalysts is clearly visible (Fig. 8). Exposure of AuMCM-41(COP) to NO + O_2 produces nitrite species characterized by the IR bands at 1739 and 1417 cm^{-1} (Fig. 8A); these are not detected on the impregnated sample (Fig. 8B). Nitrites can be formed only in the interaction with active oxygen ions. As such, ions do not exist on the activated samples (TOF-SIMS studies indicate the absence of oxygen in the gold surroundings); rather, they must be formed from the gaseous oxygen by electron transfer from the surface species (chloride ions). NO + O_2 adsorption on the impregnated sample leads to the generation of NO_2 chemisorbed species characterized by the bands at ca 1690 and 1625 cm^{-1}, with the latter chemisorbed on metal sites [9]. These species interact with propene. Subsequent admission of propene at RT leads

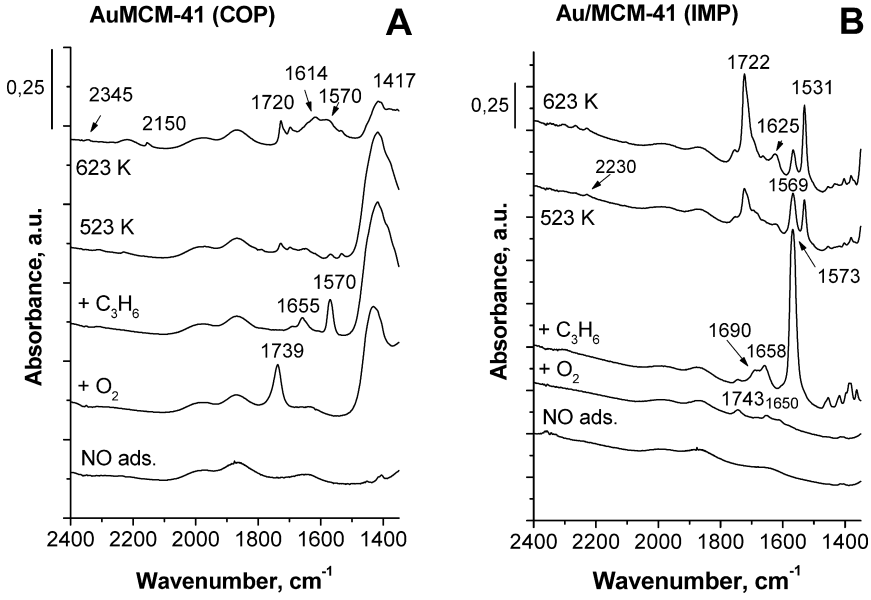

Fig. 8. FTIR spectra of AuMCM-41(COP) (A) and Au/MCM-41(IMP) (B) materials after the admission of reagents at RT in the following order: NO, O_2, C_3H_6 and heating at 523 and 623 K.

to the formation of similar IR bands on both catalysts at ca. 1690, 1650, and 1570 cm^{-1} attributed to acetone hydrogen bonded to hydroxyl groups, chemisorbed propene, and ν COO^- in acetate, respectively. However, the intensity of these bands is much higher on the impregnated sample, indicating that more gold centers are accessible for the chemisorption of these products on the impregnated material. This finding is also in agreement with the TOF-SIMS results showing that part of the gold species is surrounded by chloride and thus not exposed to the reagents and products on AuMCM-41(COP). After heating to 623 K, similar new products are observed in the IR spectra of both materials. Most of these, which are somewhat visible after heating at 523 K, include carbonates ($\sim$1530 cm^{-1}), acetone ($\sim$1720 cm^{-1}), N_2O ($\sim$2230 cm^{-1}), and CO_2 ($\sim$2345 cm^{-1}). CO ($\sim$2150 cm^{-1}) is detected only on AuMCM-41(COP). In both catalysts, the reaction route is via the formation of NO_2, which reacts with the chemisorbed propene and/or oxygenates. However, the main difference between both samples is that on AuMCM-41(COP), nitrates are formed and stored and NO_2 is released on heating, whereas on AuMCM-41(IMP), NO_2 is chemisorbed on gold species and reacts with propene and/or oxygenates.

4. Conclusion

Gold nanoparticles with different sizes were prepared in silicate MCM-41 mesoporous materials by two methods: coprecipitation in the presence of the cationic surfactant (by one-pot synthesis) and incipient wetness impregnation. The first approach led to the formation of gold in two forms: metallic (XRD, TEM, UV–vis) and surrounded (bonded) by chloride ions (TOF-SIMS). The second method generated only metallic Au species (XRD, UV–vis). TOF-SIMS measurements confirmed the presence of metallic gold in all of the samples used by ruling out the presence of oxygen in proximity to Au; AuO^-, AuO_2^- and $AuOH^-$ ions clusters were not found. The role of the surfactant in the storage of chloride ions on calcination was demonstrated by DTG/DTA analysis.

FTIR studies of the NO reduction with propene in the presence of oxygen allow characterization of the role of chloride as a promoter by taking part in electron transfer to oxygen in the NO-SCR reaction. The most important finding from this work is that chloride ions serve as a catalytically active basic species in the acetonylacetone transformation. Such activity is possible because of the weak Au–Cl interaction.

Acknowledgments

This work was partially supported by the Polish Ministry of Science and Higher Education (Grant PBZ-KBN-116/TO9/2004; 2005–2008). The authors thank Johnson Matthey for supplying the $HAuCl_4$.

References

[1] G.C. Bond, D.T. Thompson, Catal. Rev. Sci. Eng. 41 (1999) 319.
[2] G.J. Hutchings, M. Haruta, Appl. Catal. A 291 (2005) 2.
[3] B. Grzybowska-Swierkosz, Catal. Today 112 (2006) 3.
[4] M. Haruta, Catal. Today 36 (1997) 153.
[5] S. Zheng, L. Gao, Mat. Chem. Phys. 78 (2002) 512.
[6] H. Araki, A. Fukuoka, Y. Sakamoto, S. Inagaki, N. Sugimoto, Y. Fukushima, M. Ichikawa, J. Mol. Catal. A 199 (2003) 95.
[7] G. Lu, D. Ji, G. Qian, Y. Qi, X. Wang, J. Suo, Appl. Catal. A 280 (2005) 175.
[8] A. Wang, J.-H. Liu, S.D. Lin, T.-S. Lin, Ch.-Y. Mou, J. Catal. 233 (2005) 186.
[9] D.B. Akolekar, S.K. Bhargava, J. Mol. Catal. A 236 (2005) 77.
[10] M. Okumura, S. Tsubota, M. Haruta, J. Mol. Catal. A 199 (2003) 73.
[11] M. Pia Casaletto, A. Longo, A.M. Venezia, A. Martorana, A. Prestianni, Appl. Catal. A 302 (2006) 309.
[12] L. Ilieva, J.W. Sobczak, M. Manzoli, B.L. Su, D. Andreeva, Appl. Catal. A 291 (2005) 85.
[13] F. Arena, P. Famulari, N. Interdonato, G. Bonura, F. Frusteri, L. Spadaro, Catal. Today 116 (2006) 384.
[14] B. Qiao, Y. Deng, Appl. Catal. B 66 (2006) 241.
[15] J.S. Beck, J.C. Vartuli, W.J. Roth, M.E. Leonowicz, D.T. Kresge, K.D. Schmitt, C.T.W. Chu, D.H. Olson, E.W. Sheppard, S.B. McCullen, J.B. Higgins, J.L. Schlenker, J. Am. Chem. Soc. 114 (1992) 10834.
[16] C. Kan, W. Cai, Z. Li, G. Fu, L. Zhang, Chem. Phys. Lett. 382 (2003) 318.
[17] L. Fu, N.Q. Wu, J.H. Yanh, F. Qu, D.L. Johnson, M.C. Kung, H.H. Kung, V.P. Dravid, J. Phys. Chem. B 109 (2005) 3704.
[18] M. Kruk, A. Sayari, M. Jaroniec, Stud. Surf. Sci. Catal. 129 (2000) 576.
[19] R.M. Dessau, Zeolites 10 (1990) 205.
[20] J.J. Alcaraz, B.J. Arena, R.D. Gillespie, J.S. Holmgren, Catal. Today 43 (1998) 89.
[21] F. Boccuzzi, A. Chiorino, S. Tsubota, M. Haruta, Catal. Lett. 29 (1994) 225.
[22] E. Giamello, D. Murphy, G. Magnacca, C. Morterra, Y. Shioya, T. Nomura, M. Anpo, J. Catal. 136 (1992) 510.
[23] C. Kladis, S.K. Bhargava, K. Foger, D.B. Akolekar, J. Mol. Catal. A 171 (2001) 243.
[24] S.-C. Shen, S. Kawi, J. Catal. 213 (2003) 241.
[25] J.M. Garcia-Cortes, J. Perez-Ramirez, J.N. Rouzaud, A.R. Vaccaro, M.J. Illan-Gomez, C. Salinas-Martinez de Lecea, J. Catal. 218 (2003) 111.
[26] T.E. Hoost, K.A. Laframboise, K. Otto, Appl. Catal. B 7 (1995) 79.
[27] E. Finocchio, G. Busca, V. Lorenzelli, R.J. Willey, J. Catal. 151 (1995) 204.
[28] I. Sobczak, M. Ziolek, M. Nowacka, Micropor. Mesopor. Mater. 78 (2005) 103.
[29] I. Sobczak, M. Ziolek, J. Goscianska, F. Romero Saria, M. Daturi, J.M. Jablonski, Stud. Surf. Sci. Catal. 158 (2005) 1319.
[30] N. Takahashi, H. Shinjoh, T. Iijima, T. Suzuki, K. Yamazaki, K. Yokota, H. Suzuki, N. Myioshi, S. Matsumoto, T. Tanizawa, T. Tanaka, S. Tateishi, K. Kasahara, Catal. Today 27 (1996) 63.
[31] H. Mahzoul, J.F. Brilhac, P. Gilot, Appl. Catal. B 20 (1999) 47.
[32] Y. Traa, B. Burger, J. Weitkamp, Micropor. Mesopor. Mater. 30 (1999) 3.